LETTER • **OPEN ACCESS**

Even-denominator fractional quantum Hall states with spontaneously broken rotational symmetry

To cite this article: Chengyu Wang *et al* 2025 *Rep. Prog. Phys.* **88** 100501

OPEN ACCESS
IOP Publishing
Reports on Progress in Physics
Rep. Prog. Phys. **88** (2025) 100501 (10pp)
https://doi.org/10.1088/1361-6633/ae0a7f

Letter

Even-denominator fractional quantum Hall states with spontaneously broken rotational symmetry

Chengyu Wang[1,*], **A Gupta**[1], **S K Singh**[1], **C T Tai**[1], **L N Pfeiffer**[1], **K W Baldwin**[1], **R Winkler**[2] **and M Shayegan**[1,*]

[1] Department of Electrical and Computer Engineering, Princeton University, Princeton, NJ 08544, United States of America
[2] Department of Physics, Northern Illinois University, DeKalb, IL 60115, United States of America

E-mail: chengyuw@princeton.edu and shayegan@princeton.edu

Received 25 June 2025, revised 20 August 2025
Accepted for publication 23 September 2025
Published 8 October 2025

Corresponding editor: Dr Paul Mabey

Abstract
The interplay between the fractional quantum Hall effect and nematicity is intriguing as it links emerging topological order and spontaneous symmetry breaking. Anisotropic fractional quantum Hall states (FQHSs) have indeed been reported in GaAs quantum wells but only in tilted magnetic fields, where the in-plane field explicitly breaks the rotational symmetry. Here we report the observation of FQHSs with highly anisotropic longitudinal resistances in purely perpendicular magnetic fields at even-denominator Landau level (LL) fillings $\nu = 5/2$ and 7/2 in ultrahigh-quality GaAs two-dimensional hole systems. The coexistence of FQHSs and spontaneous symmetry breaking at half fillings signals the emergence of nematic FQHSs which also likely harbor non-Abelian quasiparticle excitations. By gate tuning the hole density, we observe a phase transition from an anisotropic, developing FQHS to an isotropic composite fermion Fermi sea at $\nu = 7/2$. Our calculations suggest that the mixed orbital components in the partially occupied LL play a key role in the competition and interplay between topological and nematic orders.

Supplementary material for this article is available online

Keywords: fractional quantum Hall effect, spontaneous rotational symmetry breaking, even denominator, orbitally-mixed Landau levels

* Authors to whom any correspondence should be addressed.

1. Introduction

Fractional quantum Hall states (FQHSs) are fascinating examples of interaction phenomena and topological order in condensed matter physics. Most FQHSs are observed at odd-denominator Landau level (LL) filling factors, following the Jain sequence [1–3]. These states occur in the ground-state ($N=0$) LLs where short-range Coulomb interaction dominates, and can be explained as integer quantum Hall states of weakly interacting composite fermions (CFs). The ground state at a half-filled $N=0$ LL (e.g. at $\nu=1/2$) is a compressible Fermi sea of CFs; see figure 1(a). In excited ($N\geqslant 1$) LLs, the nodal structure of the wavefunction softens the short-range Coulomb interaction, leading to a variety of exotic states that are not favored in the $N=0$ LLs [4–9]. These include FQHSs at even-denominator filling factors, first observed at a half-filled $N=1$ LL ($\nu=5/2$) of GaAs two-dimensional electron systems (2DESs) [4]. At $\nu=5/2$, the CF Fermi sea is no longer stable as the CFs undergo a Bardeen–Cooper–Schrieffer-like pairing instability and condense into a FQHS (figure 1(b)). The prime candidates for the $\nu=5/2$ FQHS are believed to host non-Abelian anyons, and be potentially useful for fault-tolerant topological quantum computation [10–14]. Even-denominator FQHSs at half fillings of the $N=1$ LLs were also reported in other material platforms, including semiconductor heterostructures [15, 16] and atomically-thin 2D materials [17–21].

In $N\geqslant 2$ LLs, stripe or electronic versions of liquid-crystal-like phases with spontaneously broken rotational symmetry emerge near half fillings [5, 6, 9, 22–27]. These states exhibit anisotropic in-plane transport coefficients with no quantized Hall plateau, and were initially predicted by Hartree–Fock theories to stem from unidirectional charge-density waves consisting of stripes with alternating integer ν [22–24, 28]. At finite temperatures, and in the presence of quantum fluctuations and disorder, the stripe order can be disrupted, leading to nematic phases (figure 1(c)) [25–27]. Alternatively, in a more general picture, nematic orders can also arise from Pomeranchuk instability of Fermi seas [29, 30].

While the vast majority of FQHSs are isotropic, FQHSs with significant longitudinal transport anisotropy were observed in the $N=1$ LL of GaAs 2DESs at $\nu=7/3$ and 5/2 in tilted magnetic fields [31, 32]. Another example of an anisotropic FQHS was reported in the half-filled $N=1$ LL of an AlAs 2DES with large band-mass anisotropy and an applied uniaxial strain [16]. These experiments suggest that FQHSs may exhibit nematic order, forming the so-called nematic FQHSs. These states are very unusual, because unlike the conventional nematic states which are understood in terms of Landau's symmetry-breaking theory and described by traditional order parameter, nematic FQHSs possess both topological and nematic order [33]. Nematicity in FQHSs has indeed attracted significant interest because of its connection to the geometrical degree of freedom in FQHSs and the intriguing coexistence of topological order with broken

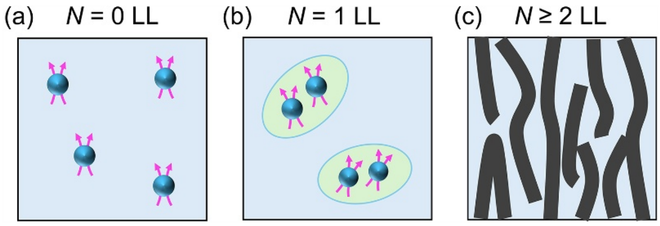

Figure 1. Ground states at half-filled LLs: (a) CF Fermi sea ($N=0$), (b) paired FQHS ($N=1$), and (c) nematic phase ($N\geqslant 2$).

symmetry [34–44]. Nematic FQHSs are theoretically predicted to exhibit a finite charge gap and a vanishing neutral gap in the long-wavelength limit [36, 37]. Anisotropic FQHSs reported in the $N=1$ LL are likely candidates for nematic FQHSs [16, 31, 32, 45]; however, their observation has until now required the application of external symmetry-breaking fields, such as in-plane magnetic fields or uniaxial strain, which *explicitly* break the rotational symmetry. In a purely perpendicular magnetic field, an unusual phase transition from a nearly isotropic FQHS to a *compressible* nematic phase, induced by hydrostatic pressure, was reported, indicating the proximity of nematic order to FQHSs [46]. However, experimental evidence for a nematic FQHS with *spontaneously* broken rotational symmetry has been lacking until now.

Here we report the observation of anisotropic FQHSs at *even-denominator* fillings $\nu=5/2$ and 7/2 in ultrahigh-quality GaAs 2D *hole* systems (2DHSs). Remarkably, these states are observed in the absence of an external symmetry-breaking field, suggesting the spontaneous rotational symmetry breaking of candidate non-Abelian FQHSs. The emergence of anisotropic FQHSs at $\nu=5/2$ and 7/2 are evinced by pronounced minima superimposed on a highly anisotropic longitudinal resistance background, accompanied by developing quantized Hall plateaus. These anisotropic FQHSs exhibit a unique combination of characteristics of both half-filled $N=1$ LL and $N\geqslant 2$ LLs, revealing the coexistence of CF paring and nematic order; see figures 1(b) and (c). We also observe qualitatively similar, albeit weaker, signatures of anisotropic FQHSs at odd-denominator fillings flanking $\nu=5/2$. At higher LL fillings ($\nu>4$), we observe numerous anisotropic phases without any FQHS features, consistent with what one would expect for high ($N\geqslant 2$) LLs.

2. Methods

We studied ultrahigh-quality 2DHSs confined to GaAs quantum wells grown on GaAs (001) substrates by molecular beam epitaxy [47–49]. Our magneto-transport measurements were performed on 4×4 mm^2 van der Pauw geometry samples, with alloyed In:Zn contacts at the four corners and side midpoints. We studied seven samples from six different wafers; see table I in supplemental material (SM) [50] for

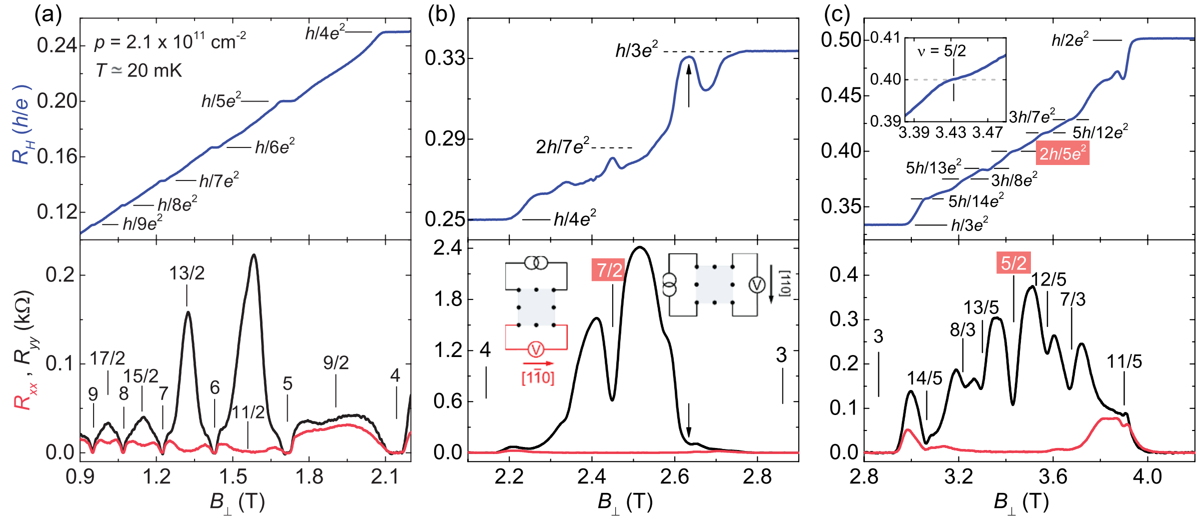

Figure 2. Hall resistance R_{H} (top panels) and longitudinal resistances R_{xx} and R_{yy} (bottom panels) for our ultrahigh-quality 2DHS; sample A. The sample has a quantum well width of 20 nm and a 2D hole density of 2.1×10^{11} cm^{-2}. Numerous anisotropic phases are observed near half fillings. (a) Anisotropic phases, without Hall plateaus, in high LLs near $\nu = 11/2$, 13/2, 15/2, and 17/2. Note that the 2DHS is isotropic at $\nu = 9/2$. (b) A developing FQHS with large transport anisotropy at even-denominator $\nu = 7/2$. Insets in the lower panel show the circuit configurations for R_{xx} and R_{yy} measurements. (c) Developing FQHSs with large transport anisotropy at even-denominator $\nu = 5/2$ and at numerous odd-denominator fillings 8/3, 13/5, 12/5, and 7/3.

sample parameters. Sample C was fitted with a Ti/Au front gate and In back gate, allowing for *in-situ* tuning of the 2D hole density. The samples were cooled in two dilution refrigerators with base temperatures of about 20 mK and 30 mK. We measured the longitudinal in-plane resistances (R_{xx} and R_{yy}) along two perpendicular directions and the Hall resistance (R_{H}) using the low-frequency, lock-in amplifier techniques.

It is worth noting that Hall measurements for anisotropic phases are challenging because of the non-uniform current distribution and significant mixing of R_{xx} signal into the Hall meausrements [9, 16, 31]. One effective method to minimize the effect of R_{xx} mixing is by averaging $|R_{xy}|$ taken for opposite polarities of $B_\perp$. Because our magnet only has the capability of applying large $B_\perp$ in one direction, we used an alternative method to minimize the effect of R_{xx} mixing [51]: we measured Hall resistances with two circuit configurations (rotated by 90°) and took their average value as R_{H}.

3. Results

Figure 2 presents Hall and longitudinal resistance data measured as a function of $B_\perp$. Longitudinal resistances R_{xx} and R_{yy} were measured along the $[1\bar{1}0]$ and [110] crystallographic directions, respectively (see insets in figure 2(b) lower part for circuit geometries). Panel (a) shows data for $\nu \geqslant 4$. We observe anisotropic phases at half fillings $\nu = 11/2$, 13/2, 15/2, and 17/2, evinced by broad dips in R_{xx} and peaks in R_{yy}. These anisotropic states resemble the stripe/nematic phases reported in GaAs 2DESs at high $N \geqslant 2$ LLs [5, 6]. Near $\nu = 9/2$, the 2DHS exhibits a nearly isotropic behavior. As we detail in the Discussion later, the isotropic phase at $\nu = 9/2$ is well explained by our LL analysis. Our data in figure 2(a) are consistent with previous reports on high-quality GaAs 2DHSs with similar parameters [52]. We note that, for $\nu > 4$, the Hall resistance R_{H} remains smooth and linear as a function of $B_\perp$ between the quantized Hall plateaus at integer fillings.

Near $\nu = 7/2$, the 2DHS exhibits strong anisotropy, with $R_{xx} \simeq 0$ and $R_{yy} \simeq 2$ kΩ (figure 2(b)). Unlike the anisotropic phases observed at higher ν, a sharp minimum in R_{yy} is observed at $\nu = 7/2$, superimposed on a resistive background. While R_{H} exhibits a complex behavior because of the non-uniform current distribution within the highly anisotropic phase, its value approaches $2h/7e^2$ to within 2% at $\nu = 7/2$. These observations suggest a developing, anisotropic FQHS at $\nu = 7/2$. At $B_\perp \simeq 2.64$ T ($\nu \simeq 3.3$), R_{H} shows a reentrant behavior towards the $h/3e^2$ plateau, indicating the emergence of a developing reentrant integer quantum Hall state. This is also supported by R_{xx} and R_{yy} data where developing minima are seen at the same $B_\perp$ position; these are more clearly resolved in measurements employing different contact configurations; see SM figure S1 [50]. Such reentrant integer quantum Hall behavior may signal the Wigner crystallization of multi-electron bubbles [7, 22, 24].

Data presented in figure 2(c) for $3 > \nu > 2$ reveal our strongest evidence for anisotropic FQHSs. At $\nu = 5/2$, a sharp R_{yy} minimum, accompanied with a developing Hall plateau centered at $R_{\mathrm{H}} = 2h/5e^2$, signals an even-denominator FQHS. Similar to what we see at $\nu = 7/2$, the 5/2 FQHS also exhibits anisotropic transport ($R_{xx} << R_{yy}$). Qualitatively similar features are seen at odd-denominator fillings $\nu = 8/3$, 13/5, 12/5, and 7/3, suggesting developing anisotropic FQHSs at these fillings also. These signatures of anisotropic FQHSs at odd- and even-denominator fillings are reproducible in multiple samples from different wafers; see figure 5 and SM figures S4 and S5 for more data [50]. Importantly, *the anisotropic FQHSs*

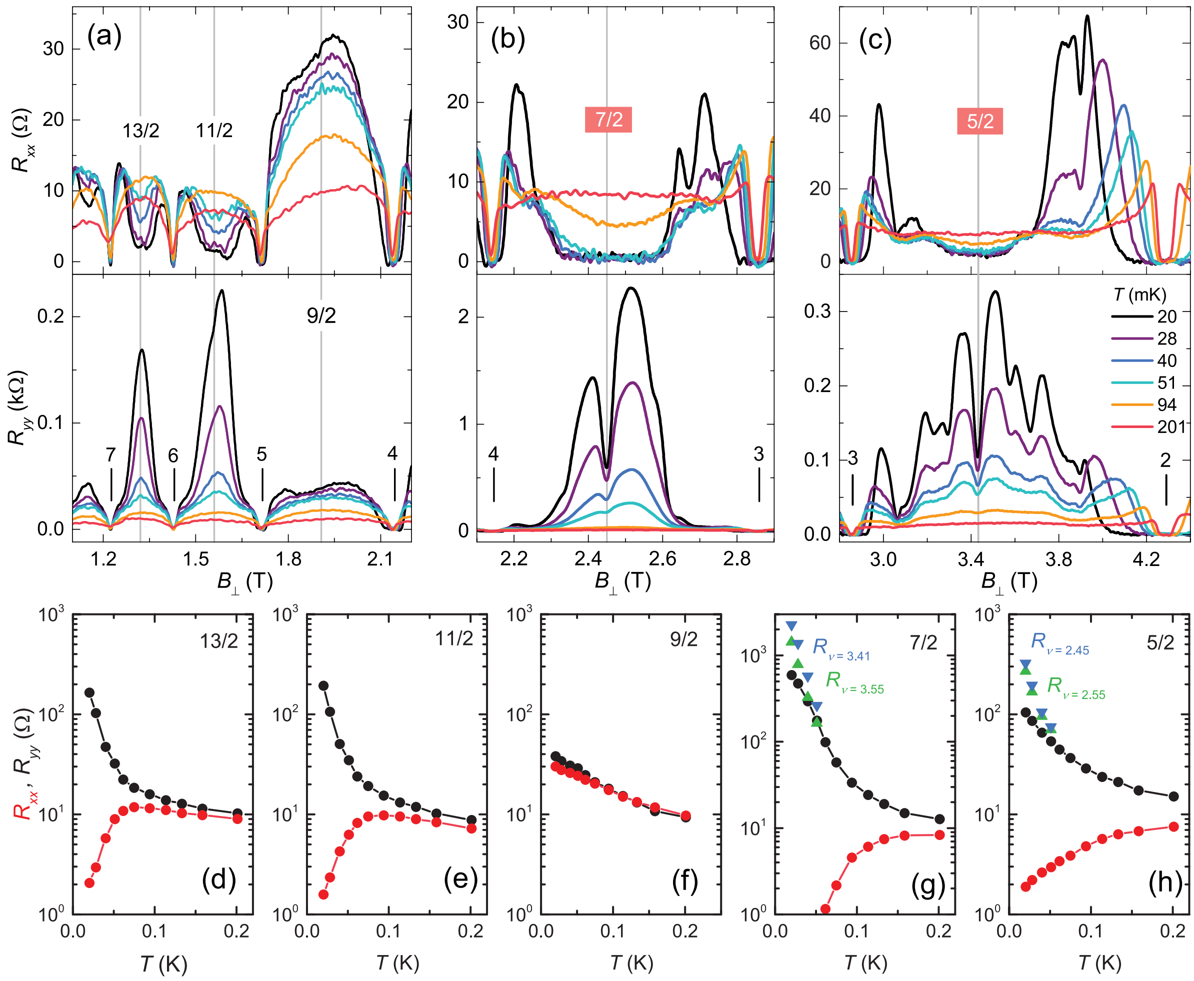

Figure 3. Temperature dependence data; sample A. (a)–(c) R_{xx} and R_{yy} vs $B_\perp$ traces taken at different temperatures for: (a) $\nu \geqslant 4$, (b) $4 \geqslant \nu \geqslant 3$, and (c) $3 \geqslant \nu \geqslant 2$. (d)–(h) Temperature dependence of R_{xx} and R_{yy} at half fillings: (d) $\nu = 13/2$, (e) 11/2, (f) 9/2, (g) 7/2, and (h) 5/2. Blue and green triangles show R_{xx} values on the flanks of $\nu = 5/2$ and 7/2 at the indicated filling factors.

in our 2DHS are observed in the absence of any external symmetry-breaking field (e.g. an in-plane magnetic field). Our results therefore provide strong evidence for spontaneously broken rotational symmetry in these FQHSs, signaling the emergence of *nematic FQHSs*.

We observe that the easy axis direction is along $[1\bar{1}0]$ for both the nematic FQHSs at $\nu = 5/2$ and 7/2 as well as for stripe/nematic phases in higher LLs (e.g. $\nu = 11/2, 13/2, \ldots$), suggesting a common rotational symmetry breaking mechanism for these states. In GaAs 2DESs, the majority of stripe/nematic phases in $N \geqslant 2$ LLs exhibit an easy axis along the [110] direction, although examples of the easy axis along $[1\bar{1}0]$ have been reported under specific conditions [53, 54]. The origin of the internal symmetry breaking field that favors a certain crystal direction over the other remains an unresolved question.

Figure 3 captures the temperature dependence of the observed nematic FQHSs and anisotropic phases. Note the differing y-axis scales in figures 3(a)–(c). The temperature dependence of R_{xx} and R_{yy} at various half fillings is further highlighted in figures 3(d)–(h). At $\nu = 9/2$ (figure 3(f)), we observe nearly isotropic transport with both R_{xx} and R_{yy} gradually increasing with decreasing T down to $T \simeq 20$ mK. In contrast to the isotropic behavior near $\nu = 9/2$, at $\nu =$ 13/2, 11/2, 7/2, and 5/2, R_{xx} and R_{yy} significantly deviate from each other and exhibit opposite trends at low T, indicating the emerging nematic order (figures 3(d), (e), (g) and (h)). Furthermore, R_{yy} minima, superimposed on a rising background, rapidly develop at $\nu = 5/2$ and 7/2. Linear fits to Arrhenius plots of the relative depth of these R_{yy} minima yield energy gap estimates of approximately 55 mK and 76 mK for the $\nu = 5/2$ and 7/2 FQHSs, respectively; see SM figure S2 for details [50]. The simultaneous emergence of FQHS and nematic order strongly supports our interpretation of these states as developing nematic FQHSs. We note that the anisotropic transport near $\nu = 7/2$ and 5/2 persists to higher temperatures ($\simeq$ 150 mK) when the FQHS features disappear, similar to what was reported for anisotropic FQHSs in tilted B [31, 32, 45].

Applying an in-plane magnetic field, $B_\parallel$, provides further insight into the nematic order at half fillings. In figures 4(a) and (b), we show R_{xx} and R_{yy} data in perpendicular and tilted B, measured for sample B at $T \simeq 30$ mK; see figure S6 in SM for more data at different θ [50]. This sample was mounted on

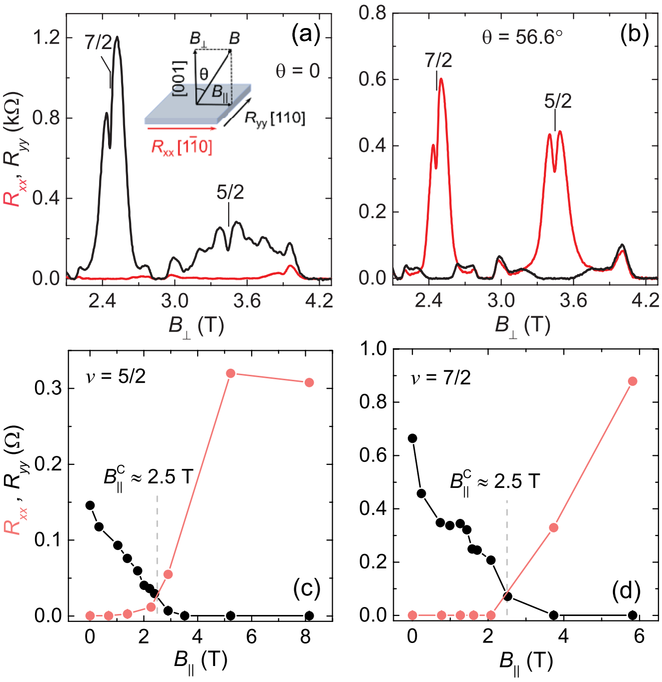

Figure 4. Impact of in-plane magnetic field ($B_{||}$) on the nematic FQHSs; sample B, $T \simeq 30$ mK. This sample has a quantum well width of 20 nm and 2D hole density of 2.1×10^{11} cm^{-2}. (a), (b) R_{xx} and R_{yy} vs $B_\perp$ traces measured at (a) zero tilt and (b) tilt angle $\theta = 56.6°$. (c), (d) R_{xx} and R_{yy} at $\nu = 5/2$ and 7/2 as a function of $B_{||}$, revealing the switching of the hard and easy axes at a critical in-plane field of $B_{||}^{C} \simeq 2.5$ T. Inset in (a): a schematic of the experimental setup. The sample is mounted on a rotating stage to support *in-situ* tilt; θ is the angle between B and $B_\perp$. By tilting the sample, a finite $B_{||} = B \times \sin\theta$ is introduced along the [1$\bar{1}$0] crystallographic direction.

a rotating stage to support *in-situ* tilt; see figure 4(a) inset. With the sample tilted, $B_{||}$ is applied along [1$\bar{1}$0] (parallel to R_{xx}) direction. At $\theta = 0$, we observe developing anisotropic FQHSs at $\nu = 5/2$ and 7/2 with $R_{xx} << R_{yy}$. At $\theta = 56.6°$, developing FQHSs survive, but the hard and easy axes of resistive anisotropy are interchanged, resulting in $R_{xx} >> R_{yy}$. We plot R_{xx} and R_{yy} at $\nu = 5/2$ and 7/2 as a function of $B_{||}$ (figures 4(c) and (d)). A critical in-plane field, $B_{||}^{C} \simeq 2.5$ T, is identified where the 2DHS becomes nearly isotropic at both $\nu = 5/2$ and 7/2. The orientation of the hard axis at large $B_{||}$ is aligned with the direction of the applied $B_{||}$, consistent with what was observed in GaAs 2DESs [32, 55–57]. Such tilt-induced anisotropy is also consistent with Hartree–Fock calculations of the unidirectional charge density wave orientation energy induced by a tilted magnetic field [58].

Next, we address the origin of the nematic FQHSs we observe at $\nu = 5/2$ and 7/2 in our 2DHSs. FQHSs at half fillings in different 2DESs are predominantly observed in the $N = 1$ LLs [4, 15, 16, 18–21]. On the other hand, the unique property of the 5/2 and 7/2 FQHSs in our 2DHSs is the spontaneous breaking of rotational symmetry. Such electronic nematic order is reminiscent of the anisotropic phases observed in higher $N \geqslant 2$ LLs in GaAs 2DESs [5, 6]. Indeed, the LLs of GaAs 2DHSs are very different compared to electrons. Because of the mixing between the heavy-hole and light-hole states in $B_\perp$ and significant spin–orbit coupling, hole LLs have a multi-orbital nature [59]. In addition, hole LLs are highly nonlinear as a function of $B_\perp$ and exhibit numerous crossings that can be tuned to coincidence with the Fermi energy, E_F [45, 60–62]. To shed light on the nature of LLs that host the nematic FQHSs, we studied the evolution of different states at half fillings with varying hole densities, and compare our data with the calculated LL fan diagrams for our sample.

Focusing first on the experimental data, in figure 5(a), we present R_{xx} and R_{yy} data for sample C at different densities. We tune the hole density from 1.13 to 1.84 (in units of 10^{11} cm^{-2}, which we use throughout the remainder of the manuscript) using front and back gates while keeping the charge distribution symmetric. Higher hole densities (>1.84) are achieved by further changing the front gate voltage only, and the charge distribution becomes slightly asymmetric. Near $\nu = 5/2$, the 2DHS is anisotropic in the density range $p = 1.13$ to 2.18. The FQHS features at $\nu = 5/2$ and 7/3 are absent at $p = 1.13$ likely because of the very low 2DHS density, and gradually develop with increasing density. No sharp transition is seen for FQHSs between $\nu = 3$ and 2. Near $\nu = 7/2$, on the other hand, the 2DHS is isotropic at low densities but becomes highly anisotropic at high densities. A sharp isotropic-to-anisotropic transition occurs at $p \simeq 1.3$. Interestingly, an R_{yy} minimum at $\nu = 7/2$ appears simultaneously with the onset of anisotropy. We also observe isotropic-to-anisotropic transitions in higher LLs, e.g. at $\nu = 11/2$. The behavior near $\nu = 9/2$ is rather different: the 2DHS is anisotropic at low densities but becomes isotropic at $p \simeq 2.0$. At $p = 2.18$, the 2DHS becomes slightly anisotropic near $\nu = 9/2$. The anisotropy at $\nu = 9/2$, however, is much weaker than that at nearby half fillings, e.g. at $\nu = 7/2$ and 11/2, where R_{xx} show deep minima. No sharp R_{yy} minimum is observed at half fillings other than 5/2 and 7/2.

4. Discussion

In order to understand the origin of the different ground states we observe at different fillings, and their evolution with density, we present calculated LL fan diagrams for our 2DHS; for more details of the LL calculations and results, see SM [50]. These LL diagrams (figures 5(b)–(d)), together with the spinor compositions of the relevant LLs (figures 5(e)–(g)) shed significant light on the emergence of the different states in the 2DHS. The calculations are performed for our 2DHS (sample C) in a purely $B_\perp$ using the multiband envelope function approximation and the 8×8 Kane Hamiltonian [59]. We also use axial approximation so that we can decompose each LL into the basis of four spinors with $s_z = \pm 3/2$ and $\pm 1/2$. The spinor composition is directly related to the orbital composition of each LL [45, 59]. In figures 5(b)–(d), we present three representative LL fan charts, calculated at different densities $p = 0.74$, 1.04, and 1.74. The three most relevant LLs (α, β, and γ) are highlighted. The spinor compositions for these LLs, shown in figures 5(d)–(f), are calculated for $p = 1.74$. Our calculations show that, for a given quantum well width, density

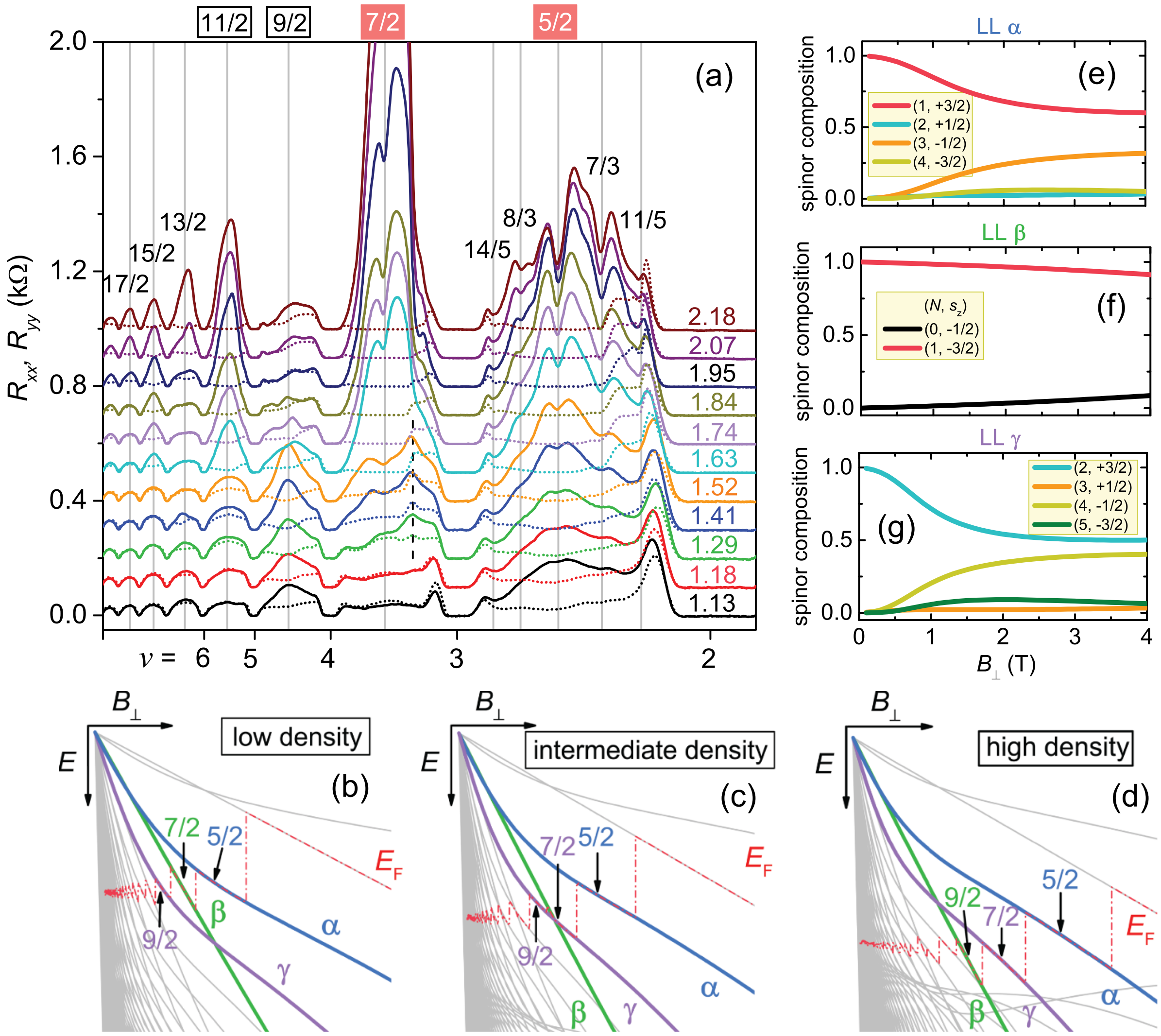

Figure 5. Gate-tuned phase transitions at half fillings; sample C, $T \simeq 20$ mK. This sample has a quantum well width of 20 nm and an as-grown density of 1.74×10^{11} cm^{-2}. (a) R_{xx} (along $[1\bar{1}0]$, dotted) and R_{yy} (along [110], solid) traces measured at different densities. Each trace is vertically shifted by 0.1 kΩ for clarity, with its corresponding 2D hole density (p), in units of 10^{11} cm^{-2}, indicated on the right. While the longitudinal transport at $\nu = 5/2$ is anisotropic in the density range of 1.13 to 2.18, transitions between isotropic and anisotropic phases are observed as a function of density at half fillings in higher LLs, e.g., at $\nu = 7/2$, 9/2, and 11/2. (b)–(d) Calculated energy vs $B_\perp$ LL fan diagrams at low ($p = 0.74$), intermediate ($p = 1.04$), and high ($p = 1.74$) densities. Three LLs ($\boldsymbol{\alpha}$, $\boldsymbol{\beta}$, and $\boldsymbol{\gamma}$ levels) of interest are highlighted. Other LLs are shown in light grey. Red dash-dotted line traces the Fermi energy E_F. Black arrows mark the positions of $\nu = 5/2$, 7/2, and 9/2. (e)–(g) Spinor compositions of $\boldsymbol{\alpha}$, $\boldsymbol{\beta}$, and $\boldsymbol{\gamma}$ LLs.

has a negligible effect on these results [50]. They are therefore representative for the whole range of densities we studied for sample C. We also note that, although there are some discrepancies, our LL calculations qualitatively capture the main features in the E vs $B_\perp$ LL fan charts, e.g. the nonlinearity in E vs $B_\perp$ and the numerous LL crossings at finite $B_\perp$.

Before we elaborate on the origin of different states at different fillings, we summarize the nature of the three LLs which are most relevant to our studies, the $\boldsymbol{\alpha}$, $\boldsymbol{\beta}$, and $\boldsymbol{\gamma}$ levels, in the magnetic field range of interest ($B_\perp > 1$ T) where we observe the different ground states in sample C for $\nu < 13/2$. As seen in figure 5(e), $\boldsymbol{\alpha}$ has mainly two dominant spinor components: $N = 1$ and $N = 3$. In contrast, $\boldsymbol{\beta}$ possesses predominantly an $N = 1$ spinor component (figure 5(f)), while $\boldsymbol{\gamma}$'s main components are $N = 2$ and $N = 4$. As we discuss below, the spinor components of $\boldsymbol{\alpha}$, $\boldsymbol{\beta}$, and $\boldsymbol{\gamma}$ can explain the evolution of the different states at different fillings in figure 5(a) to a large degree.

$\nu = 5/2$—in the density range we studied for sample C, E_F at $\nu = 5/2$ (1.9 T $< B_\perp <$ 3.6 T) remains in $\boldsymbol{\alpha}$ (figures (b)–(d)). The dominating $N = 1$ component is likely crucial for hosting the 5/2 FQHS, consistent with the fact that FQHSs at half fillings are predominantly observed in the $N = 1$ LLs [4, 16, 18–21]. The significant $N = 3$ component ($> 20\%$) at $B_\perp \geqslant 2$ T, on the other hand, is very likely the origin of nematicity near $\nu = 5/2$. We note that $\boldsymbol{\alpha}$ and $\boldsymbol{\beta}$ cross at very low $B_\perp$. Our calculations indicate that in the density range we measured for sample C, this crossing is reasonably far away from

E_F, consistent with the absence of transitions between isotropic and anisotropic behaviors near $\nu = 5/2$.

The nature of the nematic FQHS at $\nu = 5/2$ in our 2DHS is not fully clear. While the 5/2 FQHS in the $N = 1$ LL is generally associated with non-Abelian Pfaffian, anti-Pfaffian, or PH-Pfaffian topological orders [63], the coexistence of nematic order with these topological orders requires further investigation. The theoretically proposed stripe FQHS [38] and pair-density-wave FQHS [41], which can break the rotational symmetry at $\nu = 5/2$, provide potential explanations for our observations.

The developing nematic FQHSs we observe at odd-denominator fillings flanking 5/2 also warrant discussion. They emerge at $\nu = 8/3$, 13/5, 12/5, 7/3. Our LL calculations indicate that the LL (α) that hosts these states has predominantly $N = 1$ component. Theories predict that the FQHSs at $\nu = 12/5$ and 13/5 in the $N = 1$ LL may support non-Abelian Fibonacci anyonic excitations, potentially useful for universal topological quantum computing [64–66]. While a $\nu = 12/5$ FQHS has been observed in the $N = 1$ LL of GaAs 2DESs, the $\nu = 13/5$ state has remained elusive [8]. The absence of the $\nu = 13/5$ FQHS was attributed to the effect of LL mixing [66]. However, LL mixing is much larger in our 2DHS because of the larger hole effective mass, and yet our data reveal signatures of developing FQHSs at both $\nu = 13/5$ and 12/5, with significant transport anisotropy; see figure 2(c). In sample C, we also observe hints of developing FQHSs at $\nu = 12/5$ and 13/5 at $p = 2.18$; see SM figure S4 [50].

$\nu = 7/2$ and 9/2—the crossing between β and γ near E_F and their spinor compositions can qualitatively explain the transitions between isotropic and anisotropic behaviors we observe in sample C near $\nu = 7/2$ (1.3 T $< B_\perp <$ 2.6 T) and 9/2 (1.0 T $< B_\perp <$ 2.0 T). Thanks to the $N = 2$ and $N = 4$ components, anisotropic phases can be favored in γ. In contrast, anisotropic phases are not favored in β, because β does not possess any $N \geqslant 2$ components. At low densities, E_F for both $\nu = 7/2$ and 9/2 is on the lower-$B_\perp$ side of the crossing. In this case, $\nu = 7/2$ is in β while $\nu = 9/2$ is in γ. An isotropic phase near $\nu = 7/2$ and an anisotropic phase near $\nu = 9/2$ are expected. With increasing density, the crossing coincides with E_F in the range of $3 < \nu < 5$, starting from the low-ν side. At intermediate densities when E_F at $\nu = 7/2$ has moved to the higher-$B_\perp$ side of the crossing while E_F at $\nu = 9/2$ is still at the lower-$B_\perp$ side of the crossing, both $\nu = 7/2$ and 9/2 are in γ, and anisotropic phases are expected near both $\nu = 7/2$ and 9/2. At high densities, E_F at both $\nu = 7/2$ and 9/2 is on the higher-$B_\perp$ side of the crossing. In this case, $\nu = 7/2$ is in γ while $\nu = 9/2$ is in β. An anisotropic phase near $\nu = 7/2$ and an isotropic phase near $\nu = 9/2$ are expected. These are qualitatively consistent with what we observe in sample C (figure 5(a)).

We also note that the 2DHS (sample C) becomes slightly anisotropic near $\nu = 9/2$ at $p > 2.0$. However, an anisotropic behavior is not expected at high densities when E_F is on the higher-$B_\perp$ side of the crossing between β and γ. The anisotropy we observe at $p > 2.0$ in sample C is possibly associated to a different crossing between β and another LL that has $N \geqslant 2$ components.

$\nu = 11/2$, 13/2, 15/2,...—our calculations indicate that, in the density range we study for our samples, LLs at $\nu > 5$ have predominantly $N \geqslant 2$ components. This explains our observation of anisotropic phases at $\nu = 11/2$, 13/2, 15/2, and 17/2 in sample A (figure 2(a)) and at $p > 2.0$ in sample C (figure 5(a)). At low densities (e.g. $p = 1.13$), the absence of anisotropic phases at these fillings is likely because that such phases are very fragile and may require lower temperatures and disorder at lower densities.

It is worth noting that the agreement between our data and our LL calculations is qualitative. There are some discrepancies if we make quantitative comparisons. For example, in our LL calculations, we predict that E_F at $\nu = 7/2$ crosses from β to γ at $p \simeq 1.0$, and that E_F at $\nu = 9/2$ crosses from γ to β at $p \simeq 1.3$. In our experiment, however, the isotropic-to-anisotropic transition at $\nu = 7/2$ occurs at $p \simeq 1.3$, and the anisotropic-to-isotropic transition at $\nu = 9/2$ occurs at $p \simeq 1.9$. Similar quantitative discrepancies were also seen in several previous studies of crossings between other LLs in GaAs 2DHSs [60–62]. Although the origin of these discrepancies is unclear, it appears that the calculations always predict the crossings to occur at lower $B_\perp$ compared to experimental observations.

While our calculated LLs, including their compositions, capture some key experimental features, puzzles still remain. First, our LL calculations cannot explain the observed nematic FQHS at $\nu = 7/2$. Our calculations indicate that the LL (γ) that hosts the $\nu = 7/2$ nematic FQHS only has $N \geqslant 2$ components, but does not have any $N = 1$ component. This is consistent with the absence of FQHSs at odd-denominator fillings that may be favored in an $N = 1$ LL. The emergence of a nematic FQHS at $\nu = 7/2$ in a $N = 2$-dominant LL suggests a distinct origin compared to the nematic FQHS at $\nu = 5/2$. Another puzzling observation relates to the temperature dependence of the anisotropic phases at $\nu = 5/2$ and 7/2 in tilted B. In the $N \geqslant 2$ LLs of GaAs 2DESs, the anisotropic phases typically become more robust in tilted B as compared to in purely $B_\perp$ [57]. Unexpectedly, we find that at $\theta = 66.2°$, the anisotropic phases at $\nu = 5/2$ and 7/2 turn isotropic at much lower T ($\simeq$75 mK; see figure S7 in SM [50]) compared to what we observe in purely $B_\perp$ ($\gtrsim$150 mK; see figures 3(g) and (h)).

A phase transition from an isotropic CF Fermi sea to a highly anisotropic FQHS was reported at $\nu = 3/2$ in GaAs 2DHSs under tilted B [45]. While such an anisotropic FQHS is likely also associated with a LL possessing multiple spinor components, there are some key differences: (i) the large in-plane B in tilted B explicitly breaks the rotational symmetry and favors anisotropic phases at $\nu = 3/2$, in stark contrast to the spontaneous rotational symmetry breaking we observe here at $\nu = 5/2$ and 7/2. (ii) Our observation of nematic FQHSs at $\nu = 5/2$ and 7/2, as well as the phase transitions at $\nu = 7/2$ and 9/2 show clear correlation with the calculated LL spinor components and crossings. However, similar calculations for LLs and their spinor components in tilted B are not available because of computational challenges. This hinders a quantitative LL analysis of the anisotropic FQHS at $\nu = 3/2$ which was only seen in tilted B.

5. Conclusion

Our observation of nematic FQHSs with spontaneously broken rotational symmetry at both even- and odd-denominator ν, as well as the transitions between isotropic and anisotropic phases, highlight the rich physics in the quantum Hall regime of ultrahigh-quality GaAs 2DHSs. The effects of heavy-hole light-hole and spin-orbit couplings render GaAs hole LLs multi-orbital, making them unique systems that support coexisting topological and nematic orders. Furthermore, the tunability of LL components and crossings provide useful platforms for realizing and engineering novel, exotic, interaction phenomena, and studying phase transitions between distinct strongly correlated phases.

Our work also highlights the crucial role of sample quality in the exploration of emergent many-body phenomena. Improvements in atomically-thin 2D materials, such as graphene-based systems and transition metal dichalcogenides, have also made available new types of material platforms for studies of FQHSs and other many-body phases [17–21]. These new materials have significantly expanded the scope of FQHS research by introducing different tuning knobs and probing techniques, enabling exciting observations [67, 68]. Among a variety of materials, the modulation-doped GaAs/AlAs quantum wells yet remain a leading platform for the discovery of new emergent phenomena and for potential applications, thanks to their record-high transport mobility [47–49]. An additional key advantage of the GaAs/AlAs system is the large sample size ($\sim$25 mm^2), about 10^6 times larger than devices made of exfoliated 2D flakes.

Data availability statement

The data cannot be made publicly available upon publication because the cost of preparing, depositing and hosting the data would be prohibitive within the terms of this research project. The data that support the findings of this study are available upon reasonable request from the authors.

Supplementary data 1 available at https://doi.org/10.1088/1361-6633/ae0a7f/data1.

Acknowledgments

We acknowledge support by the National Science Foundation (NSF) Grant No. DMR 2104771 for measurements, and the Gordon and Betty Moore Foundation's EPiQS Initiative (Grant No. GBMF9615 to L N P) for sample fabrication. Our measurements were partly performed at the National High Magnetic Field Laboratory (NHMFL), which is supported by the NSF Cooperative Agreement No. DMR 2128556, by the State of Florida, and by the DOE. This research was funded in part by QuantEmX grant from Institute for Complex Adaptive Matter and the Gordon and Betty Moore Foundation through Grant GBMF9616 to C W, A G, S K S, and C T T. We thank A Bangura, G Jones, R Nowell and T Murphy at NHMFL for technical assistance, and J K Jain for illuminating discussions.

ORCID iDs

Chengyu Wang 0009-0004-0059-8345
A Gupta 0000-0001-5350-3443
S K Singh 0009-0002-1114-5988

References

[1] Tsui D C, Stormer H L and Gossard A C 1982 Two-dimensional magnetotransport in the extreme quantum limit *Phys. Rev. Lett.* **48** 1559
[2] Jain J K 1989 Composite-fermion approach for the fractional quantum Hall effect *Phys. Rev. Lett.* **63** 199
[3] Jain J K 2007 *Composite Fermions* (Cambridge University Press)
[4] Willett R, Eisenstein J P, Störmer H L, Tsui D C, Gossard A C and English J H 1987 Observation of an even-denominator quantum number in the fractional quantum Hall effect *Phys. Rev. Lett.* **59** 1776
[5] Lilly M P, Cooper K B, Eisenstein J P, Pfeiffer L N and West K W 1999 Evidence for an anisotropic state of two-dimensional electrons in high Landau levels *Phys. Rev. Lett.* **82** 394
[6] Du R R, Tsui D C, Stormer H L, Pfeiffer L N, Baldwin K W and West K W 1999 Strongly anisotropic transport in higher two-dimensional Landau levels *Solid State Commun.* **109** 389
[7] Eisenstein J P, Cooper K B, Pfeiffer L N and West K W 2002 Insulating and fractional quantum Hall states in the first excited Landau level *Phys. Rev. Lett.* **88** 076801
[8] Kumar A, Csáthy G A, Manfra M J, Pfeiffer L N and West K W 2010 Nonconventional odd-denominator fractional quantum Hall states in the second Landau level *Phys. Rev. Lett.* **105** 246808
[9] Fu X, Shi Q, Zudov M A, Gardner G C, Watson J D, Manfra M J, Baldwin K W, Pfeiffer L N and West K W 2020 Anomalous nematic states in high half-filled Landau levels *Phys. Rev. Lett.* **124** 067601
[10] Moore G and Read N 1991 Nonabelions in the fractional quantum Hall effect *Nucl. Phys. B* **360** 362
[11] Nayak C, Simon S H, Stern A, Freedman M and Sarma S D 2008 Non-Abelian anyons and topological quantum computation *Rev. Mod. Phys.* **80** 1083
[12] Banerjee M, Heiblum M, Umansky V, Feldman D E, Oreg Y and Stern A 2018 Observation of half-integer thermal Hall conductance *Nature* **559** 205
[13] Halperin B I and Jain J K (eds) 2020 *Fractional Quantum Hall Effects: New Developments* (World Scientific)
[14] Willett R L, Shtengel K, Nayak C, Pfeiffer L N, Chung Y J, Peabody M L, Baldwin K W and West K W 2023 Interference measurements of non-Abelian $e/4$ & Abelian $e/2$ quasiparticle braiding *Phys. Rev. X* **13** 011028
[15] Falson J, Maryenko D, Friess B, Zhang D, Kozuka Y, Tsukazaki A, Smet J H and Kawasaki M 2015 Even-denominator fractional quantum Hall physics in ZnO *Nat. Phys.* **11** 347
[16] Hossain M S, Ma M K, Chung Y J, Pfeiffer L N, West K W, Baldwin K W and Shayegan M 2018 Unconventional anisotropic even-denominator fractional quantum Hall state in a system with mass anisotropy *Phys. Rev. Lett.* **121** 256601

[17] Ki D K, Fal'ko V I, Abanin D A and Morpurgo A F 2014 Observation of even denominator fractional quantum Hall effect in suspended bilayer graphene *Nano Lett.* **14** 2135
[18] Zibrov A A, Kometter C, Zhou H, spanton E M, Taniguchi T, Watanabe K, Zaletel M P and Young A F 2017 Tunable interacting composite fermion phases in a half-filled bilayer-graphene Landau level *Nature* **549** 360
[19] Li J I A, Tan C, Chen S, Zeng Y, Taniguchi T, Watanabe K, Hone J and Dean C R 2017 Even-denominator fractional quantum Hall states in bilayer graphene *Science* **358** 648
[20] Huang K, Fu H, Hickey D R, Alem N, Lin Xi, Watanabe K, Taniguchi T and Zhu J 2022 Valley isospin controlled fractional quantum Hall states in bilayer graphene *Phys. Rev. X* **12** 031019
[21] Shi Q, Shih E-M, Gustafsson M V, Rhodes D A, Kim B, Watanabe K, Taniguchi T, Papić Z, Hone J and Dean C R 2020 Odd- and even-denominator fractional quantum Hall states in monolayer WSe_2 *Nat. Nanotechnol.* **15** 569
[22] Koulakov A A, Fogler M M and Shklovskii B I 1996 Charge density wave in two-dimensional electron liquid in weak magnetic field *Phys. Rev. Lett.* **76** 499
[23] Fogler M M, Koulakov A A and Shklovskii B I 1996 Ground state of a two-dimensional electron liquid in a weak magnetic field *Phys. Rev. B* **54** 1853
[24] Moessner R and Chalker J T 1996 Exact results for interacting electrons in high Landau levels *Phys. Rev. B* **54** 5006
[25] Fradkin E and Kivelson S A 1999 Liquid-crystal phases of quantum Hall systems *Phys. Rev. B* **59** 8065
[26] Fradkin E, Kivelson S A, Manousakis E and Nho K 2000 Nematic phase of the two-dimensional electron gas in a magnetic field *Phys. Rev. Lett.* **84** 1892
[27] Fradkin E, Kivelson S A, Lawler M J, Eisenstein J P and Mackenzie A P 2010 Nematic Fermi fluids in condensed matter physics *Annu. Rev. Condens. Matter Phys.* **1** 153
[28] See also Sammon M *et al* 2019 Resistivity anisotropy of quantum Hall stripe phases *Phys. Rev. B* **100** 241303
[29] Oganesyan V, Kivelson S A and Fradkin E 2001 Quantum theory of a nematic Fermi fluid *Phys. Rev. B* **64** 195109
[30] Lee K, Shao J, Kim E-A, Haldane F D M and Rezayi E H 2018 Pomeranchuk instability of composite Fermi liquids *Phys. Rev. Lett.* **121** 147601
[31] Xia J, Eisenstein J P, Pfeiffer L N and West K W 2011 Evidence for a fractionally quantized Hall state with anisotropic longitudinal transport *Nat. Phys.* **7** 845
[32] Liu Y, Hasdemir S, Shayegan M, Pfeiffer L N, West K W and Baldwin K W 2013 Evidence for a $\nu = 5/2$ fractional quantum Hall nematic state in parallel magnetic fields *Phys. Rev. B* **88** 035307
[33] Wen X G 1995 Topological orders and edge excitations in fractional quantum Hall states *Adv. Phys.* **44** 405
[34] Haldane F D M 2011 Geometrical description of the fractional quantum Hall effect *Phys. Rev. Lett.* **107** 116801
[35] Mulligan M, Nayak C and Kachru S 2011 Effective field theory of fractional quantized Hall nematics *Phys. Rev. B* **84** 195124
[36] Maciejko J, Hsu B, Kivelson S A, Park Y and Sondhi S L 2013 Field theory of the quantum Hall nematic Transition *Phys. Rev. B* **88** 125137
[37] You Y, Cho G Y and Fradkin E 2014 Theory of nematic fractional quantum Hall states *Phys. Rev. X* **4** 041050
[38] Wan X and Yang K 2016 Striped quantum Hall state in a half-filled Landau level *Phys. Rev. B* **93** 201303(R)
[39] Yang B, Hu Z-X, Lee C H and Papić Z 2017 Generalized pseudopotentials for the anisotropic fractional quantum Hall effect *Phys. Rev. Lett.* **118** 146403
[40] Regnault N, Maciejko J, Kivelson S A and Sondhi S L 2017 Evidence of a fractional quantum Hall nematic phase in a microscopic model *Phys. Rev. B* **96** 035150
[41] Santos L H, Wang Y and Fradkin E 2019 Pair-density-wave order and paired fractional quantum Hall fluids *Phys. Rev. X* **9** 021047
[42] Yang B 2020 Microscopic theory for nematic fractional quantum Hall effect *Phys. Rev. Res.* **2** 033362
[43] Ye D, Jiang C-X and Hu Z-X 2024 Fractional quantum Hall nematics at $\nu = 7/3$ in a tilted magnetic field *Phys. Rev. B* **110** 165123
[44] Pu S, Balram A C, Taylor J, Fradkin E and Papić Z 2024 Microscopic model for fractional quantum Hall nematics *Phys. Rev. Lett.* **132** 236503
[45] Wang C, Gupta A, Chung Y J, Pfeiffer L N, West K W, Baldwin K W, Winkler R and Shayegan M 2023 Highly anisotropic even-denominator fractional quantum Hall state in an orbitally coupled half-filled Landau level *Phys. Rev. Lett.* **131** 056302
[46] Samkharadze N, Schreiber K A, Gardner G C, Manfra M J, Fradkin E and Csáthy G A 2016 Observation of a transition from a topologically ordered to a spontaneously broken symmetry phase *Nat. Phys.* **12** 191
[47] Chung Y J, Villegas Rosales K A, Baldwin K W, Madathil P T, West K W, Shayegan M and Pfeiffer L N 2021 Ultra-high-quality two-dimensional electron systems *Nat. Mater.* **20** 632–7
[48] Chung Y J, Wang C, Singh S K, Gupta A, Baldwin K W, West K W, Winkler R, Shayegan M and Pfeiffer L N 2022 Record-quality GaAs two-dimensional hole systems *Phy. Rev. Mater.* **6** 034005
[49] Gupta A, Wang C, Singh S K, Baldwin K W, Winkler R, Shayegan M and Pfeiffer L N 2024 Ultraclean two-dimensional hole systems with mobilities exceeding 10^7 cm^2/Vs *Phys. Rev. Mater.* **8** 014004
[50] See supplemental material for additional data and discussions.
[51] Goldman V J, Shayegan M and Tsui D C 1988 Evidence for the fractional quantum Hall state at $\nu = 1/7$ *Phys. Rev. Lett.* **61** 881
[52] Manfra M J, de Picciotto R, Jiang Z, Simon S H, Pfeiffer L N, West K W and Sergent A M 2007 Impact of spin-orbit coupling on quantum Hall nematic phases *Phys. Rev. Lett.* **98** 206804 (In this work, a nearly isotropic phase at $\nu = 9/2$ and anisotropic phases at $\nu = 7/2$, 11/2 and 13/2 were reported. No FQHS was osbserved at $\nu = 5/2$ and 7/2, although a shallow minimum in longitudinal resistance (in the high resistance direction) was seen at 5/2.)
[53] Zhu J, Pan W, Stormer H L, Pfeiffer L N and West K W 2002 Density-induced interchange of anisotropy axes at half-filled high Landau levels *Phys. Rev. Lett.* **88** 116803
[54] Pollanen J, Cooper K B, Brandsen S, Eisenstein J P, Pfeiffer L N and West K W 2015 Heterostructure symmetry and the orientation of the quantum Hall nematic phases *Phys. Rev. B* **92** 115410
[55] Lilly M P, Cooper K B, Eisenstein J P, Pfeiffer L N and West K W 1999 Anisotropic states of two-dimensional electron systems in high Landau levels: effect of an in-plane magnetic field *Phys. Rev. Lett.* **83** 824
[56] Pan W, Du R R, Stormer H L, Tsui D C, Pfeiffer L N, Baldwin K W and West K W 1999 Strongly anisotropic electronic transport at Landau level filling factor $\nu = 9/2$ and $\nu = 5/2$ under a tilted magnetic field *Phys. Rev. Lett.* **83** 820
[57] Cooper K B, Lilly M P, Eisenstein J P, Pfeiffer L N and West K W 2002 Onset of anisotropic transport of two-dimensional electrons in high Landau levels: possible isotropic-to-nematic liquid-crystal phase transition *Phys. Rev. B* **65** 241313(R)

[58] Jungwirth T, MacDonald A H, Smrčka L and Girvin S M 1999 Field-tilt anisotropy energy in quantum Hall stripe states *Phys. Rev. B* **60** 15574

[59] Winkler R 2003 *Spin-Orbit Coupling Effects in Two-Dimensional Electron and Hole Systems* (Springer)

[60] Liu Y, Hasdemir S, Kamburov D, Graninger A L, Shayegan M, Pfeiffer L N, West K W, Baldwin K W and Winkler R 2014 Even-denominator fractional quantum Hall effect at a Landau level crossing *Phys. Rev. B* **89** 165313

[61] Lupatini M, Knüppel P, Faelt S, Winkler R, Shayegan M, Imamoglu A and Wegscheider W 2020 Spin reversal of a quantum Hall ferromagnet at a Landau level crossing *Phys. Rev. Lett.* **125** 067404

[62] Ma M K, Wang C, Chung Y J, Pfeiffer L N, West K W, Baldwin K W, Winkler R and Shayegan M 2022 Robust quantum Hall ferromagnetism near a gate-tuned $\nu = 1$ Landau level crossing *Phys. Rev. Lett.* **129** 196801

[63] Ma K K W, Peterson M R, Scarola V W and Yang K 2024 Fractional quantum Hall effect at the filling factor $\nu = 5/2$ *Encyclopedia of Condensed Matter Physics* 2nd edn, ed T Chakraborty (Academic) pp 324–65

[64] Read N and Rezayi E 1999 Beyond paired quantum Hall states: parafermions and incompressible states in the first excited Landau level *Phys. Rev. B* **59** 8084

[65] Zhu W, Gong S S, Haldane F D M and Sheng D N 2015 Fractional quantum Hall states at $\nu = 13/5$ and 12/5 and their non-Abelian nature *Phys. Rev. Lett.* **115** 126805

[66] Pakrouski K, Troyer M, Wu Y-L, Sarma S D and Peterson M R 2016 Enigmatic 12/5 fractional quantum Hall effect *Phys. Rev. B* **94** 075108

[67] Tsui Y-C, He M, Hu Y, Lake E, Wang T, Watanabe K, Taniguchi T, Zaletel M P and Yazdani A 2024 Direct observation of a magnetic-field-induced Wigner crystal *Nature* **628** 287

[68] Hu Y *et al* 2025 High-resolution tunnelling spectroscopy of fractional quantum Hall states *Nat. Phys.* **21** 716